*Semiconductor Physics, Quantum Electronics & Optoelectronics, 2013. V. 16, N 1. P. 43-47.*

PACS 43.35.Ei, 81.05.Cy, 81.40.-z

# Properties of the crystalline silicon strained via cavitation impact

**R.K. Savkina**
*V. Lashkaryov Institute of Semiconductor Physics, NAS of Ukraine,*
*41, prospect Nauky, 03028 Kyiv, Ukraine; e-mail: r_savkina@isp.kiev.ua*

**Abstract.** Properties of crystalline silicon under acoustic cavitation have been investigated. The cavitation impact was initiated by focusing a high-frequency (1–6 MHz) acoustic wave in liquid nitrogen. AFM, optical and scanning electron microscopy methods as well as energy dispersive X-ray spectroscopy were used to analyze morphology and chemical composition of semiconductor surface. Surface structurization and chemical transformations induced at the solid-liquid interface was observed. The XRD investigation pointed to stresses in the semiconductor lattice induced by the cavitation effect. A standard procedure of photoresponse spectroscopy was employed prior to and after sonication and pointed to an essential photosensitivity rise of the silicon target. The mechanisms involved during Si sonication have been discussed.

**Keywords:** crystalline silicon, acoustic cavitation, X-ray spectroscopy, photoresponse spectroscopy, atomic force microscopy.

Manuscript received 30.10.12; revised version received 05.12.12; accepted for publication 26.01.13; published online 28.02.13.

## 1. Introduction

Semiconductor manufacturing employs strain engineering to enhance device performances. For example, significant enhancement in the hole mobility in a SiGe-on-insulator metal-oxide-semiconductor field-effect transistor was achieved using the lateral-strain-relaxation process [1]. In recent years, substrate- and/or process-induced strained channels have been successfully integrated into MOSFETs in order to enhance carrier mobility [2, 3]. The use of various strain engineering techniques has been reported by many prominent microprocessor manufacturers, including AMD, IBM, and Intel.

Silicon is an industrial key material that has been widely considered in microelectronic technology, integrated circuits, and optoelectronic devices. The effect of strain on carrier transport has been known in bulk silicon for more than 50 years [4], however, only starting from the 90-nm technology node the strain engineering has been incorporated into manufacturing the advanced CMOS transistors.

It was shown that strain engineering for CMOS applications is done at high temperatures [5]. In this paper, a low-temperature approach by introducing stress on silicon using cavitation impacts is presented. In the previous work, the suitable cavitation conditions to cause modification of the gallium arsenide surface up to the microscale pattern formation as well as a change in the chemical composition of semiconductor have been successfully established [6]. It was also reported the results of studies of complex structures formed on semiconductor surface (Si and GaAs) as a result of exposing it to acoustic cavitation near liquid-solid interface [7]. In this investigation, the author uses cavitations' impact to introduce mechanical stresses on silicon to modify its properties.

## 2. Experimental

Materials used in this study were boron-doped (100)-oriented *p*-type silicon wafers of diameter about 76.2-mm grown by the liquid-encapsulated Czochralski method. The samples were cut into (5×5)mm$^2$ squares and were cleaned for 10 min in ethanol and then in distilled water. All the samples were treated by the cavitation impact in cryogenic liquid such as nitrogen.

To activate cavitation, the high frequency system (1 to 6 MHz) with a focused energy resonator described elsewhere [6, 7] was used. The semiconductor target was placed inside the acoustically driven copper cell filled with technical liquid nitrogen where the cavitation

processing was initiated. The maximal value of pressure was about ~8 bars in the focus of the acoustic system. The collapsing of the cavitation bubbles caused a shock wave and/or microjets on the semiconductor surface, thereby causing a suitable effect.

All the processed surfaces were examined after fixed cavitation intervals using AFM, as well as optical and scanning electron microscopy. The structural features were observed by X-ray diffraction (XRD). The XRD analysis was performed in a classic reflection geometry using Cu $K_\alpha$ radiation ($\lambda_{CuK\alpha 1}$ = 0.15406 nm). A standard procedure of photoresponse spectroscopy was employed prior to and after sonication.

## 3. Results and discussion

It was found that sonication of the silicon samples results in the essential photosensitivity increase both for an integrated value and for the absolute maximum (see Fig. 1). The measured value of the photovoltaic response was about 10 mV at the light power density $\leq 0.01\,\mathrm{W}\cdot\mathrm{mm}^{-2}$. The initial spectrum is a selective peak with the spectral position of the red boundary that corresponds to the silicon bandgap $E_g$ = 1.158 eV (300 K). After sonication, the short-wave shift (0.11 eV) of the red boundary occurs.

### *3.1. Silicon surface characterization using AFM, SEM and optical microscopy*

AFM topographic measurements allow one to monitor the morphological evolution of the sonicated silicon samples. The initial surface was found to be totally flat, devoid of defects, with a measured roughness lower than 1 nm. The roughness was determined on a few randomly chosen areas of (40×40) $\mu m^2$. Sonication of silicon samples leads to surface structurization. The characteristic dimension of the structures on the semiconductor surface depends on the exposure parameters (duration, acoustic power) and can be controlled by tuning the acoustic frequency.

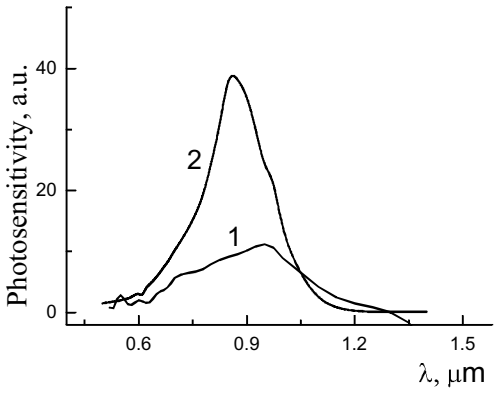


**Fig. 1.** Relative spectral photosensitivity of the typical silicon sample: (1) – initial, (2) – after sonication.

Some optical and SEM images of silicon samples exposed to acoustic cavitation are shown in Figs 2a to 2d. All the samples exhibited negligible surface modification up to at least the first 5 min. After about 10 min of testing time, optical (Fig. 2a) and electron (Fig. 2b) microscopy reveals small pits on the surface. After 15…30 min of sonication, the character of surface modification becomes more complex. Together with small pits, rings about 5 μm in diameter are formed (Figs 2c and 2d).

It was revealed that the increase of acoustic intensity under the same frequency enlarges the effective size of the zone of liquid undergone to cavitation and thereby results in some increase in the impact region. Prolonged sonication (up to 1 h) at the sufficient acoustic intensity leads to generation of large microstructured areas. It was found the creation of the dendritic structures that are seen to accumulate on the microstructured surface of silicon samples (see Fig. 2e). It was also found that the increase in a processing frequency changes both the species and the size (from submicron- to nanoscale dimension) of the structures formed on the surface [7].

### *3.2. Silicon characterization using X-ray diffraction method*

The silicon samples microstructured by the cavitation impact were measured using the X-ray diffraction method. Fig. 3 gives the XRD result of the Si(100) sample before and after cavitation treatment. The initial XRD pattern reveals only the Si(400) diffraction peak that indicates (100) orientation of the silicon wafer. The presence of a higher intensity background within the range of 2Θ = 20…30 degrees in the XRD pattern for the initial state denotes the existence of a small amount of amorphous phase on the Si surface.

XRD pattern obtained after cavitation treatment has more complex structure. It is worth to note an essential increase in the Si(400) diffraction peak intensity as well as splitting of this line. On the right of the intense peak at 2Θ = 69.27° corresponding to the reflection from the (400) plane of the silicon, the intense peak at 2Θ = 69.74° was detected. Moreover, the peak with intensity $0.5I_{400}$ is observed between mentioned peaks, i.e. (400) reflection of the silicon is resolved into two peaks due to $K_{\alpha 1}$ and $K_{\alpha 2}$ rays (see Fig. 3).

Using the strong (400) peak in the XRD pattern, the lattice parameters of the processed silicon is calculated to be $a_0$ = 5.4248 Å. These values are about 0.2% lower than the results for initial sample ($a_0$ = 5.4344 Å). Besides, the splitting up to 0.01 Å (*d*-spacing) was detected for (400) peak.

A new peaks related with formation of some compounds are observed in XRD pattern, too. In particular, it was found formation of silicates and sulfates of alkali metals (see Fig. 3). The broad diffraction peak appearing at 2Θ = 21.5º shows formation of $SiO_2$ nanocrystals. Initial and processed

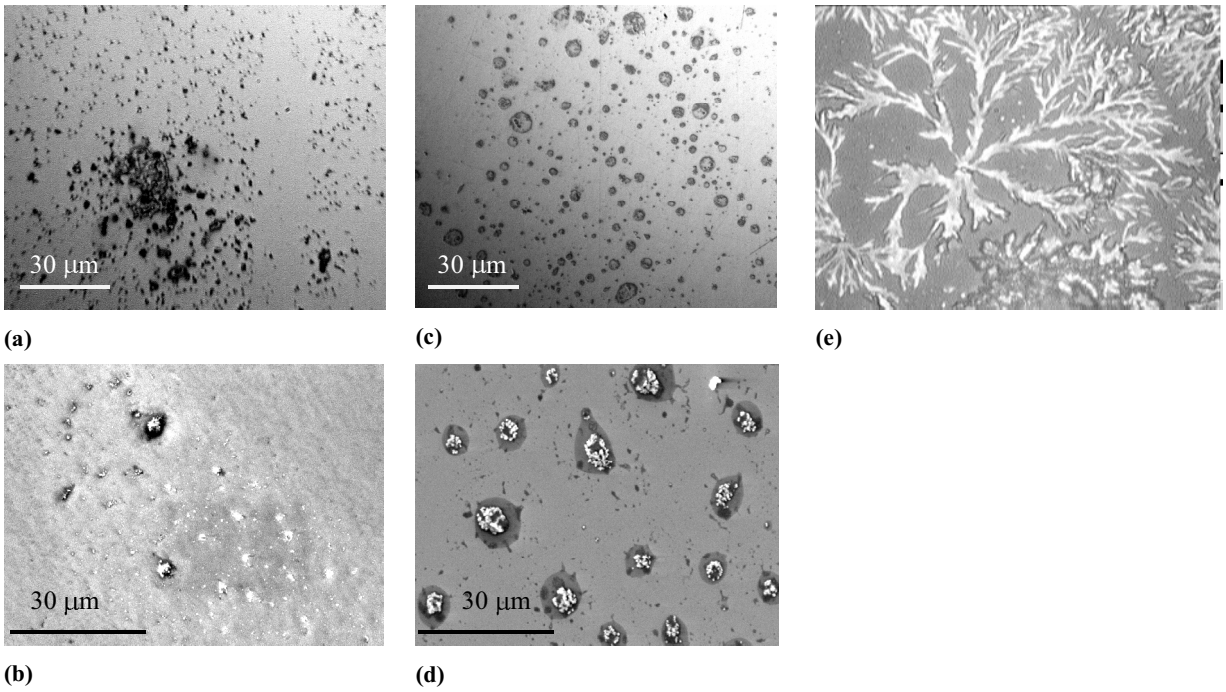


**Fig. 2.** Optical (a, c) and SEM (b, d) images of Si samples exposed to acoustic cavitation in liquid nitrogen at 6 MHz; (e) – optical image of the dendritic structures.

samples were characterized by means of energy dispersive X-ray spectroscopy (EDS). The chemical composition was studied on a numerous randomly chosen areas of (40×40) $\mu m^2$. For the processed samples, in addition to silicon peak EDS analysis indicated high oxygen (up to 10%) concentration as well as peaks corresponding to the following elements: Na, K, Ca, P, S and Cl with the weight percent within $1-2$ %.

It is well known that such change in XRD patterns as lines splitting as well as line broadening and shift can be related with lattice strain. In our case, the upward shift of the silicon (400) peak, in comparison to the initial position of it, indicates tensile stress in the semiconductor lattice after cavitation processing. It can be estimated as $\sigma = \frac{E\varepsilon}{(1-\nu)}$, where $\varepsilon = \Delta a / a_s$, $E$ is the Young modulus, $\nu$ – Poisson's ratio. This gives a localized residual stress approximately 1.55 GPa, which corresponds to a strain close to 1.19%. The stress that causes the XRD peak splitting is mainly due to defect and chemical inhomogeneity in silicon after sonication.

### *3.3. Analysis of cavitation-induced phenomena in silicon target*

Thus, the experimental study demonstrates formation of microstructures as well as change in the chemical composition on the silicon surface after cavitation processing. Besides, the XRD investigation reveals stresses in the semiconductor lattice induced by the cavitation effect. It is natural that an essential rise of photosensitivity in the semiconductor target has been ascribed to observed phenomena. Let us consider this assumption.

The photosensitivity of the semiconductor crystal can be characterized by the photocurrent, $I_{PC}$, which is proportional to the optical absorption coefficient and given by the expression:

$$I_{PC} = e\Phi\, \alpha\, d\, \eta\, [(\mu\tau)_e + (\mu\tau)_h],$$

where $e$ is the electron charge, $\Phi$ – photon flux, $\alpha$ – optical absorption coefficient, $\eta$ – quantum efficiency, $(\mu\tau)_e$ and $(\mu\tau)_h$ are the mobility–lifetime products of electrons and holes, respectively.

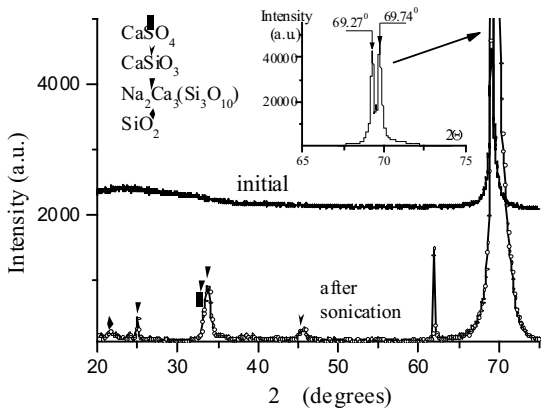


**Fig. 3.** XRD spectrum of the silicon sample exposed to cavitation impacts. The crystallographic database WWW-MINCRYST [12] was used for identification of peaks.

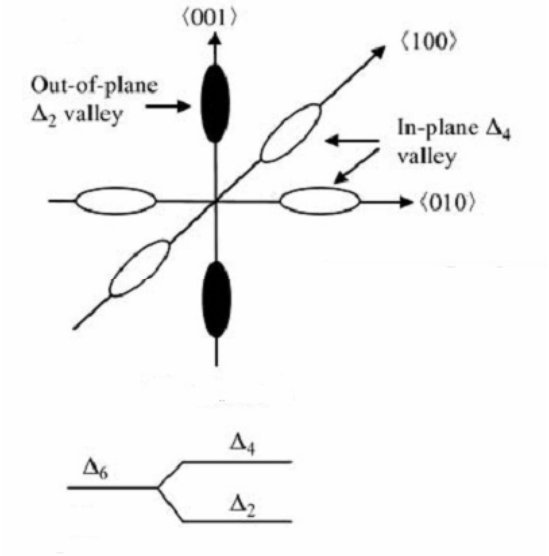


**Fig. 4.** Conduction band structure for electrons in bulk silicon without strain and the energy level split by strain.

Flat silicon is fairly reflective even in the visible wavelength range, limiting the sensitivity of silicon photodetectors and the efficiency of silicon solar cells. Such methods as anisotropic wet etching, reactive ion etching, laser processing are applied for silicon surface structurization. As a result, reducing the reflection of visible light increases the visible absorbance, making silicon surface more photosensitive. For example, microstructured silicon with roughly 90% light absorption at wavelengths from the near ultraviolet to the near infrared was developed using laser-chemical etching [8]. Thus, the photosensitivity rise of the silicon target can be related *inter alia* with the surface micro-structurization due to the cavitation processing.

Another factor had an effect on the photosensitivity of the semiconductor crystal is a recombination process. For silicon, recombination through an energy state created within the bandgap by a localized state (Shockley–Read–Hall (SRH) process) is the dominant recombination mechanism. The recombination rate depends on the number of defects present in material, so gettering of the silicon wafer resulting from the cavitation impact [9, 10] can result in the decrease in the rate of SRH recombination and carrier lifetime (as well as diffusion length) increasing. It is necessary to note that the gettering of silicon occurs after sonication, evidently, when the samples are heated up to the room temperature, and the process of diffusion is more probable.

At last, applying advantageous of strain engineering modifies the band structure of silicon in a way that the carrier mobility is increased. The carrier mobility depends on the carrier effective mass ($m^*$) and carrier relaxation ($\tau$) time as $\mu = q\tau / m^*$. In unstrained Si, the constant energy surfaces of the six conduction-band valleys ($\Delta_6$) have an ellipsoidal shape (Fig. 4), where the semi-axes of the ellipsoid are characterized by the longitudinal ($m_l^* = 0.92\, m_0$, parallel to an axis) and transverse ($m_t^* = 0.19\, m_0$, perpendicular to an axis) electron masses. The effective mass of electrons can be obtained by averaging contributions from six degenerate valleys as

$$m^* = \left[\frac{1}{6}\left(\frac{2}{m_l^*} + \frac{4}{m_t^*}\right)\right]^{-1}.$$

Applying strain on Si removes the degeneracy in the four in-plane valleys ($\Delta_4$) and the two out-of-plane valleys ($\Delta_2$) of the conduction band minimum by splitting, as it is shown in Fig. 4. This can result in two effects favorable of higher mobility for in-plane transport: the $\Delta_2$ valleys are preferentially occupied by electrons, and the other is suppression of inter-valley scattering between $\Delta_4$ and $\Delta_2$ due to energy splitting [11].

## 4. Conclusion

To summarize, the properties of the silicon samples exposed to cavitation impacts have been studied. High-intensity sonication of the silicon samples in liquid nitrogen was shown to induce changes of physical, chemical, and structural properties of semiconductor surface. The experimental study demonstrates formation of microstructures as well as change of chemical composition on the silicon surface. Besides, the XRD peak splitting is observed, which evidences the complex stress state induced by acoustic cavitation in the Si crystal structure. It was found that sonication of silicon has resulted in the photosensitivity increase. The photosensitivity rise of the silicon target can be related with the surface micro-structurization, gettering the silicon wafer as well as modification of the band structure due to the cavitation processing of silicon. These phenomena are caused by interaction between the acoustically generated bubbles and silicon surface.

## Acknowledgment

The author is grateful to Dr. A. Smirnov and Dr. T. Kryshtab for comments and many stimulating discussions.

*References*

1. T. Irisawa, T. Numata, T. Tezuka, K. Usuda, N. Hirashita, N. Sugiyama, E. Toyoda, and S. Takagi, High Performance Uniaxially Strained SGOI pMOSFETs Fabricated by Lateral Strain Relaxation Technique on Globally Strained SGOI // *IEEE Trans. Electron Devices*, **53**, p. 2809-2815 (2006).
2. C.K. Maiti and G.A. Armstrong, *Applications of Silicon Germanium Heterostructure Devices*. Inst. of Physics, UK, 2001.

3. S. Thompson, M. Armstrong, C. Auth, S. Cea, R. Chau, G. Glass, A logic nanotechnology featuring strained-silicon // *IEEE Electron Dev. Lett.* **24**, p. 191-193 (2004).
4. C. Smith, Piezoresistance effect in germanium and silicon // *Phys Rev.* **94**, p. 42-49 (1954).
5. B. Ghyselen, Strain engineering in SOI-type materials for future technologies // *Mat. Sci. Eng. B*, **124-125**, p. 16-23 (2005).
6. R.K. Savkina, A.B. Smirnov, Nitrogen incorporation into GaAs lattice as a result of the surface cavitation effect // *J. Phys. D: Appl. Phys.*, **43**, 425301 (2010).
7. R.K. Savkina, Structurization of semiconductor surfaces induced by ultrasound // *Functional Materials*, **19**(1), p. 38-43 (2012).
8. C. Wu, C.H. Crouch, L. Zhao, J.E. Carey, R. Younkin, J.A. Levinson, E. Mazur, R.M. Farrell, P. Gothoskar, and A. Karger, Near-unity below-band-gap absorption by microstructured silicon // *Appl. Phys. Lett.* **78**, p. 1850 (2001).
9. H. Soyama, S. Saitoh, D.O. Macodiyo and M. Koyanagi, C-V characteristics of backside damage gettering introduced by a cavitating jet in silicon wafer // *Proc. the 2nd Intern. Symposium on Mechanical Science based on Nanotechnology,* 2005, p. 85-88.
10. M. Virot, R. Pflieger, E.V. Skorb, J. Ravaux, T. Zemb, and H. Mohwald, Crystalline silicon under acoustic cavitation: From mechanoluminescence to amorphization // *J. Phys. Chem. C*, **116**, 15493 (2012).
11. S.I. Takagi, J.L. Hoyt, J.J. Welser, and J.F. Gibbons, Comparative study of phonon-limited mobility of two-dimensional electrons in strained and unstrained Si metal-oxide-semiconductor field-effect transistors // *J. Appl. Phys.* **80**, p. 1567 (1996).
12. http://database.iem.ac.ru/mincryst.